Biochimica et Biophysica Acta, 681 (1982) 504–511
Elsevier Biomedical Press

BBA 41152

PHOTOELECTROCHEMICAL PROPERTIES OF ELECTRODES COATED WITH PHOTOACTIVE-MEMBRANE VESICLES ISOLATED FROM PHOTOSYNTHETIC BACTERIA

MICHAEL SEIBERT and MICHAEL W. KENDALL-TOBAIS

Solar Energy Research Institute, Golden, CO 80401 (U.S.A)*

(Received December 21st, 1981)
(Revised manuscript received June 16th, 1982)

Key words: Bacterial photosynthesis; Chromatophore; Electron transfer; Membrane vesicle; Photoelectrochemical cell; (Rps. sphaeroides)

Chromatophore and sphericle vesicles, isolated from the photosynthetic bacterium, *Rhodopseudomonas sphaeroides* R-26, were dried as a film on tin oxide electrodes, and their response to red light was examined in a liquid-junction, photoelectrochemical cell. Steady-state photocurrents demonstrate that electron transfer must occur across both the SnO_2/chromatophore interface and the chromatophore film itself. The photoelectrochemical cell functions only when the chromatophore quinone pool is oxidized and cytochrome c_2 is reduced. Proton transport is not involved. Coated SnO_2 electrodes act as photocathodes instead of photoanodes, which is the case for uncoated SnO_2. The addition of electron carriers to photoelectrochemical cells incorporating chromatophore- and sphericle-coated electrodes suggest that factors other than the orientation of the reaction center within the vesicle membrane play an important part in governing the net electrical responses. A model is proposed to explain how electron transport occurs across a vesicle-coated electrode.

Introduction

A number of photosynthetic components have been incorporated into photoelectrochemical cells of various types and observed to generate photovoltages and photocurrents that can be measured directly [1,2]. Some investigators have demonstrated that intact vesicles can elicit photoelectrochemical responses: (a) in compartmentalized photoelectrochemical cells with reaction center/phospholipid vesicles attached to planar lipid membranes, or with chloroplasts aspirated onto membrane filters separating the two compartments [3,4]; (b) in photoelectrochemical cells containing electrodes coated with chloroplasts or algae [5,6]; or (c) in photogalvanic cells containing chloroplasts or chromatophores [7,8]. In attempting to understand these systems, we need to know how a potential can be generated across the diameter of a vesicle when, for example, in the case of isolated bacterial chromatophores, the reaction centers are all oriented such that light-induced primary electron flow occurs from the inside of the vesicle to the outside.

This paper will examine the electrochemical properties of isolated chromatophores and inverted chromatophores (sphericles) which have been dried as films on transparent tin oxide electrodes. Since these electrodes are capable of generating steady-state photocurrents in a photoelectrochemical cell, the light-induced charge separation that occurs across the total thickness of chromato-

Abbreviations: BChl, bacterochlorophyll; Tricine, *N*-tris(hydroxymethyl)methylglycine; FCCP, carbonyl cyanide *p*-trifluoromethoxyphenylhydrazone.

* A Division of the Midwest Research Institute and operated for the U.S. Department of Energy under contract EG-77-C-01-4042.

phores in the film must be due to electron transport across both the chromatophore membrane and also between chromatophore vesicles. The following reactions summarize the relevant transmembrane electron-transport pathways [9]. Reaction 1 occurs by direct electron transfer from $BChl_2$ to Q and secondary electron donation from cytochrome c_2 to $BChl_2$:

$$\text{cytochrome } c_2 - BChl_2 - Q \xrightarrow{h\nu} \text{cytochrome } c_{2^+} - BChl_2 - Q^- \quad (1)$$

Reaction 2 occurs via cyclic electron transport back across the membrane through cytochrome *b*:

$$\text{cytochrome } c_2^+ - BChl_2 - Q^- \xrightarrow{\text{dark}} \text{cytochrome } c_2 - BChl_2 - Q \quad (2)$$

Reaction 2 is normally coupled to proton transport and ATP production in the organism. Cytochrome c_2 is physically located on the inside of the isolated chromatophore vesicle membrane; the bacteriochlorophyll dimer, primary electron donor ($BChl_2$) is located within the membrane; and the ubiquinone (Q) acceptor is located towards the outside of the chromatophore membrane.

Proton transport across the vesicle [3,8] cannot explain the results we observe. As will be demonstrated, electron transport alone is sufficient to explain the observed photoeffects, and we have developed a model to explain our results.

Materials and Methods

Chromatophore and sphericle vesicles were isolated from the purple nonsulfur photosynthetic bacterium *Rhodopseudomonas sphaeroides* R-26 (a mutant strain of ATH 2.4.1 lacking highly unsaturated carotenoids) which was grown photoheterotrophically. Fresh, washed cells were broken in a French pressure cell at 20000 lb/inch^2 and centrifuged at $14000 \times g$ for 15 min. The supernatant was then centrifuged at $200000 \times g$ for 100 min, and the blue-green chromatophore part of the pellet was resuspended in 10 mM Tris-HCl (pH 8). Sphericles, spheroplast-derived vesicles with the reaction centers oriented in the opposite direction to those in chromatophores, were prepared essentially by the method of Takemoto and Bachmann [10] and also resuspended in 10 mM Tris-HCl (pH 8).

Reaction center orientation in both chromatophores and sphericles was assayed by determining the percentage of reaction centers rereduced by externally added reduced cytochrome *c* in the presence of antimycin A and after light-induced bleaching of reaction center BChl. In chromatophores the rereduction of reaction centers by external cytochrome *c* was about 15% of the total reaction center content, while in sphericles it was greater than 85%. About 85% of the chromatophore reaction centers were rereducible by internally bound cytochrome *c*. Sphericles contained no cytochrome *c*. Thus, in both cases reation center orientation was 85% or greater. Chromatophores were used either fresh or for up to 3 months after storage at −20°C; sphericles were used fresh unless otherwise indicated. Both were transferred to H_2SO_4-cleaned, antimony-doped, SnO_2 (an n-type semiconductor from Corning Glass Works, Corning, New York; see Ref. 2) electrodes by dipping the electrodes directly into concentrated (approx. 2 mM BChl) suspensions of vesicles. Excess liquid was removed from the lower end of the electrodes, and they were allowed to dry for 1 h in the dark under ambient conditions.

The anaerobic experimental photoelectrochemical cell (Fig. 1) was bubbled with high purity argon ($[O_2] < 1$ ppm). It consisted of a vesicle-coated, SnO_2 working electrode; a platinum counter electrode; and electrolyte containing 50 mM Tricine (pH 7 unless otherwise stated), 100 mM Na_2SO_4, and redox reagents as indicated in the text. All chemicals were of the highest commercially available purity. In addition, the cell also contained a salt bridge leading to a saturated calomel electrode. Three-electrode studies were performed using an EG&G Model 173 potentiostat (Princeton, New Jersey). In these studies the working electrode could be poised at different potentials without affecting the redox potential of the electrolyte. Redox potentiometry was accomplished as described previously (Ref. 11 and Fig. 5 of this paper) except that photovoltages, measured between the working and counter electrodes, were monitored instead of absorbance changes. Redox potentials (E_h) were measured between the platinum counter and saturated calomel electrodes but are stated in reference to the normal hydrogen electrode at pH 7.0 ($E_{h,7}$) unless otherwise indi-

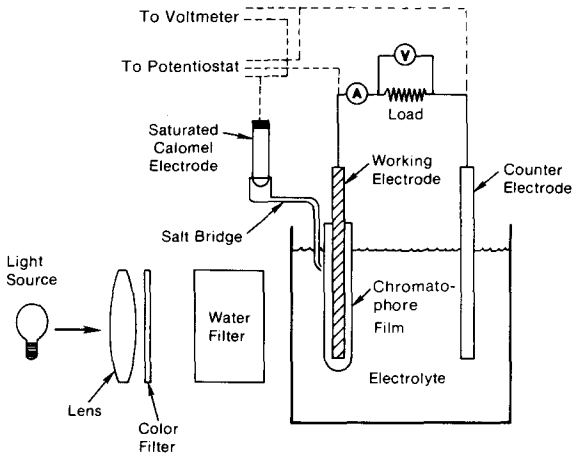

Fig. 1. The experimental photoelectrochemical cell. The redox potential of the electrolyte was obtained by measuring the voltage between the platinum counter electrode and the saturated calomel reference electrode. A potentiostat was used to poise the potential of the working electrode during three-electrode experiments.

cated. Steady-state red light ($\lambda > 600$ nm) from a 35-W Unitron tungsten lamp (Unitron Instruments, Inc., Woodbury, New York) and a Corning CS 2-62 plus a 7-cm water filter combination elicited the reported photoresponses. Single turnover flashes (3 μs) from a modified PRA Model 6100B pulsed xenon source (London, Ontario) were also passed through a Corning CS 2-62 filter. Two-electrode photoresponses are either open-circuit photovoltages or short-circuit photocurrents measured using a Keithley Instruments Model 177 multimeter (Cleveland, OH). Fast photocurrent kinetics were measured using a Nicolet Instruments Corp. (Madison, WI) Explorer 206 digital oscilloscope and a Keithley 427 current amplifier (Cleveland, OH).

Results

Fig. 2 shows the photovoltage and photocurrent kinetics generated by a chromatophore-coated SnO_2 electrode. The initial peak effects relax to a nonzero, steady-state value. We have also observed (data not shown) that for the same chromatophore preparation the photovoltage and photocurrent vary with the film thickness. In Fig. 3 the peak photocurrent is plotted as a function of the potential imposed on the chromatophore-coated working electrode using the three-electrode configuration illustrated in Fig. 1.

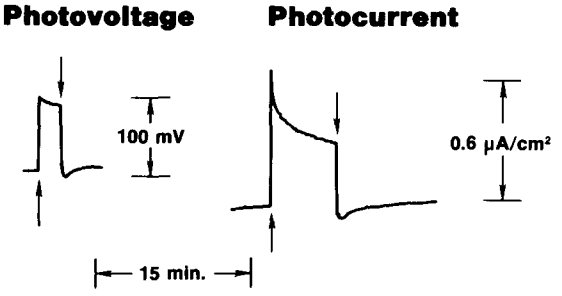

Fig. 2. Photovoltages and photocurrents generated by a chromatophore-coated SnO_2 electrode in a photoelectrochemical cell. The electrolyte ($E_{h,7} = +203$ mV) contained 10 mM hydroquinone and the light irradiance was 5 mW/cm^2. Upward-facing arrows indicate light on and downward-facing arrows denote light off. An increase in photovoltage or photocurrent corresponds to electron transfer from the working electrode to the electrolyte (a photocathodic current).

The photovoltages and photocurrents (two-electrode) generated in a photoelectrochemical cell by electrodes coated with either chromatophores or sphericles are shown in Table I (A and B). The photoeffects generated by chromatophore elec-

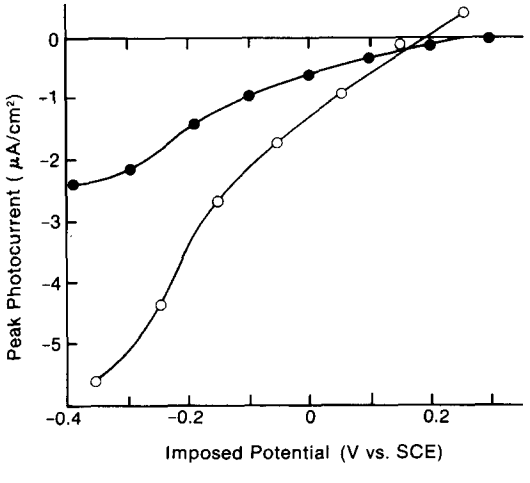

Fig. 3. The peak photocurrent generated between a chromatophore-coated working and counter electrode as a function of the potential imposed on the working electrode with respect to the reference electrode. A negative photocurrent corresponds to electron transport from the chromatophore film to the electrolyte. The electrolyte contained 10 mM hydroquinone ($E_{h,7} = +203$ mV). The light irradiance was 68 mW/cm^2 (○——○) and 5 mW/cm^2 (●——●). SCE, saturated calomel electrode.

TABLE I

PHOTOEFFECTS GENERATED BY CHROMATOPHORE- AND SPHERICLE-COATED TIN OXIDE ELECTRODES IN A PHOTOELECTROCHEMICAL CELL

The first values indicated are peak values while those in parentheses are steady-state values (see Fig. 2). The electrolyte contained 10 mM hydroquinone (pH 7). The thicknesses of the films were adjusted such that the absorbance at 800 nm was the same. In Expt. C, horse heart cytochrome *c* (cyt *c*) was added to the sphericle suspension (approx. 3 : 1 cytochrome to reaction center) before fabrication of the electrode. In Expt. D, 1,4-naphthoquinone (NQ) was added to the electrolyte of B to a concentration of 100 μM and the data taken after $1\frac{1}{2}$ h to insure equilibration. In Expt. E, antimycin A (AA) was added to the electrolyte of an Expt. B replicate to 10 μM and the data taken after $1\frac{1}{2}$ h. Higher than normal antimycin concentrations were used to ensure penetration of the chromatophore film. In Expt. F, antimycin A and 1,4-naphthoquinone were both added to the electrolyte of Expt. C and the data taken after $1\frac{1}{2}$ h. Red light irradiance ($\lambda > 600$ nm), 50 mW/cm^2; $E_{h,7} = 210$–215 mV.

Exp.	Electrode and electrolyte additions	Open-circuit photovoltage (mV)	Short-circuit photovoltage (μA/cm^2)
A	Chromatophore-coated	48(25)	0.30(0.10)
B	Sphericle-coated	0.5(0)	0.01(0)
C	Sphericle + cyt *c*	11(8)	0.23(0.05)
D	Sphericle + NQ	6(0)	0.05(0)
E	Sphericle + AA	12.5(7)	0.03(0.01)
F	Sphericle + cyt *c* + NQ + AA	42(16)	0.33(0.04)

trodes are much larger than those generated by sphericle-coated electrodes. However, spherices do not contain cytochrome c_2, one of the components present in the cyclic electron-transport chain of chromatophores. Thus, Table I (C and D) demonstrates that the addition of natural or artificial electron carriers to sphericles before fabrication of an electrode, or to the electrolyte itself, can result in substantial increases in the photovoltages and photocurrents. However, if 1,4-naphthoquinone-2-sulfonate is substituted for 1,4-naphthoquinone, no increase in photoresponse is observed.

The involvement of the cyclic electron-transport pathway in the mechanism of electron transport across sphericle or chromatophore films is explored in Table I (E) and Table II where antimycin A, an inhibitor of electron transport between cytochrome *b* and cytochrome c_2, is added to the system. Both the peak and steady-state photovoltages and photocurrents increase after ad-

TABLE II

THE RELATIVE CHANGE IN PEAK PHOTORESPONSE UPON ADDITION OF ANTIMYCIN A AND NAPHTHOQUINONE TO CHROMATOPHORE- AND SPHERICLE-COATED ELECTRODES

Chromatophores, sphericles, or a sphericle/cytochrome *c* mixture (approx. 3 : 1 cytochromes per reaction center) were dried as films on tin oxide electrodes and used in the photoelectrochemical cell of Fig. 1. The electrolyte contained 10 mM hydroquinone. After control values were obtained, either 10 μM antimycin A (AA), 100 μM 1,4-naphthoquinone (NQ), or both were added to the electrolyte and the indicated peak photoresponses were measured as a fraction of the control value. Red light irradiance 50 mW/cm^2; $E_{h,7} = 205$–215 mV. PV, photovoltage; PI, photocurrent.

Electrode	Photoeffect	No addition	AA	NQ	AA + NQ
Chromatophore	PV	1.0	1.5	1.5	1.6
	PI	1.0	2.0	2.0	1.5
Sphericle	PV	1.0	25	12	35
	PI	1.0	2.1	3.5	3.32
Sphericle + cytochrome *c*	PV	1.0	2.8	1.2 [a]	3.7
	PI	1.0	1.8	0.7 [a]	1.4

[a] The sphericle sample was frozen (−20°C) for 2 months before use.

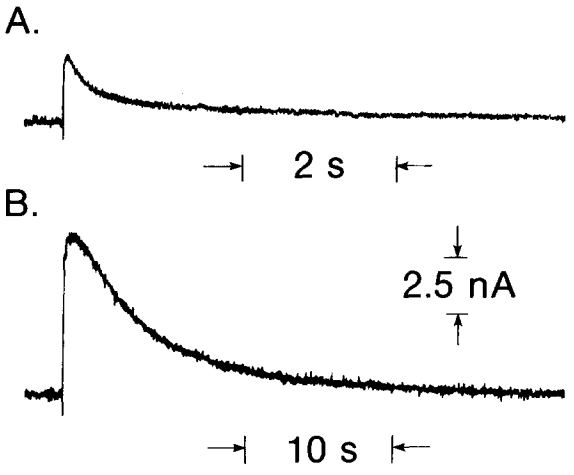

Fig. 4. Short-circuit photocurrent kinetics produced by chromatophore-coated electrodes exposed to a saturating, single turnover flash. (A) Control; (B) plus antimycin A (10 μM). The electrolyte contained 10 mM hydroquinone.

dition of the inhibitor, although the relative effects on the steady-state responses are greatest in the case of sphericles lacking cytochrome *c* (chromatophore data not shown). Fig. 4 shows an increase in both the peak value and the decay lifetime of the short-circuit photocurrent generated by a single turnover flash when antimycin is added to the electrolyte of a photoelectrochemical cell containing a chromatophore electrode. The rise time observed on a faster time scale in both cases was about 18 ms. Similar results were noted for the photovoltage although the kinetics were somewhat slower. The presence of cytochrome *c*, 1,4-naphthoquinone and antimycin A in the sphericle system (Table I, E) results in greater photoresponses than those caused by the presence of each individually. However, in the case of chromatophores (Table II), the effects of 1,4-naphthoquinone and antimycin A are not additive. This is also true for the photocurrent when sphericles contain cytochrome *c*. All photoresponses which we have observed correspond to electron transport from the vesicle film to the electrolyte. It should be noted at this point that proton transport does not contribute to the photoresponses because the addition of the uncoupler FCCP plus the ionophore valinomycin to the electrolyte of photoelectrochemical cells containing chromatophore electrodes does not significantly influence the photoeffects (data not shown).

TABLE III

THE INFLUENCE OF SODIUM SULFATE ON THE PEAK PHOTOEFFECTS GENERATED BY A CHROMATOPHORE-COATED TIN OXIDE ELECTRODE.

The electrolyte (pH 7.6; $E_h = -85$ mV vs. saturated calomel electrode) contained 10 mM EDTA and 300 μM $FeCl_3$. The light irradiance was 56 mW/cm^2.

Salt concentration (mM)	Open-circuit photovoltage (mV)	Short-circuit photocurrent (μA/cm^2)
0	166	2.52
10	157	2.18
100	154	2.50
1000	18	1.03

The chemical properties of the electrolyte greatly influence the photoresponses produced by chromatophore-coated electrodes in the photoelectrochemical cell. A case in point is the pH. With 10 mM hydroquinone ($E_{m,7} = +280$mV) in the electrolyte, the peak photovoltage was maximum at pH 7 while the peak photocurrent increased with pH from 6 to 9. However, in 10 mM EDTA/300 μM $FeCl_3$ ($E_{m,7} = +119$ mV), the peak photovoltage was maximum at pH 9 and above while the peak photocurrent was not strongly influenced by pH between 7 and 11. This may be due in part to different pK values of the mediators.

Table III shows the effect of salt concentration on the system using EDTA/$FeCl_3$ as the redox agent. Even though high salt concentrations are normally used in semiconductor photoelectrochemical cells, there is little effect until the salt concentration approaches 1 M. Protein denaturation probably occurs at this high concentration, since the initial photoeffects are not regenerated when the salt concentration is lowered from 1 M back to 10 mM. The photoresponses we have observed using EDTA/$FeCl_3$ appear to be higher than those observed for hydroquinone, but we have not attempted to optimize the concentrations in either redox system.

Fig. 5 shows the effects of electrolyte redox potential on the peak photovoltage generated by the system. At the high-potential end of the cor-

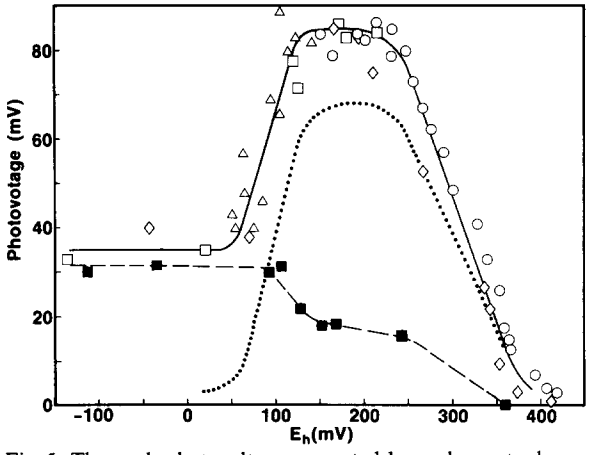

Fig. 5. The peak photovoltage generated by a chromatophore-coated SnO_2 electrode as a function of electrolyte redox potential prior to illumination. The raw data are denoted by open symbols and the solid line. The dashed line is a control experiment in which the chromatophore-coated SnO_2 electrode was autoclaved (eliminating biologically associated photochemistry). Therefore, in this case the observed photovoltage is a system artifact due perhaps to the direct photoreduction of the redox dyes with Tricine as the donor [4]. The dotted line, the difference between the solid and dashed lines, is the true photovoltage generated by the chromatophore film. The electrolyte contained 50 mM Na_2SO_4 and the pH was 7.0. The redox potential was adjusted by injecting small amounts of potassium ferricyanide or sodium dithionite into the anaerobic cell. The light irradiance was 56 mW/cm^2 and was saturating. Redox mediators and initial concentrations in the electrolyte; (□, △, or ■) 300 μM $FeCl_3$/10 mM EDTA, 50 μM phenazine ethosulfate, 33 μM duroquinone, 50 μM 2-hydroxy-1,4-naphthoquinone, 50 μM sodium anthraquinone-2,6-disulfonate, 50 μM sodium anthraquinone-2-sulfonate, and 50 μM benzyl viologen; (○) 150 μM hydroquinone, 50 μM diaminodurene, 50 μM sodium 1,2-naphthoquinone-4-sulfonate, 300 μM $FeCl_3$/10 mM EDTA; (◇) 30 μM potassium ferricyanide, 50 μM hydroquinone, 50 μM sodium 1,2-naphthoquinone-4-sulfonate, 300 μM $FeCl_3$/10 mM EDTA, 50 μM 1,4-naphthoquinone, 33 μM duroquinone, 50 μM 2-hydroxy-1,4-naphthoquinone. Each of the above symbols denotes a separate run with a different electrode.

rected curve (dotted), the photovoltage decreases in a one-electron reaction with a redox midpoint potential (pH 7) of +310 mV. At the low-potential end, the photovoltage decreases in a two-electron reaction with a midpoint potential equal to +90 mV.

Discussion

Photovoltages and photocurrents generated by the photoelectrochemical cells described in this paper are clearly due to light absorbed by the vesicle film rather than light effects attributable to the SnO_2, since SnO_2 is transparent in the visible and is not sensitive to red light [1,2]. Steady-state photocurrents demonstrate that electron transfer must occur across both the SnO_2 electrode/chromatophore interface and the chromatophore film itself and that capacitive-coupling phenomena are not involved, at least not in the steady state. Furthermore, the results of Fig. 3 demonstrate that SnO_2, which normally acts as a photoanode, acts as a photocathode when coated with a chromatophore film.

Although Expts. A and B of Table I suggest that the orientation of the reaction center within the photosynthetic vesicle membrane, and hence the direction of light-induced electron flow across the membrane, determines the magnitude of the photoeffects observed, Expt. C of Table I shows that the addition of cytochrome *c* to cytochrome-depleted sphericles can partially regenerate the extent of the photoeffects observed in chromatophores (which contain cytochrome c_2). Further regeneration occurs upon the addition of antimycin A and 1,4-naphthoquinone. Therefore, the orientation of the reaction center is not of primary importance in vesicle-coated systems.

The importance of the electrochemical properties of the electrolyte is emphasized in Fig. 5 (dotted curve), which demonstrates that the photoelectrochemical cell functions between +90 and +310 mV. The characteristics of the diminution of the photovoltage on the low-potential side corresponds to the reduction of the Q pool and those on the high-potential side to the oxidation of cytochrome c_2 [9]. Thus, in order for photoresponses to be observed, cytochrome c_2 must act as a donor and the quinone pool must act as an acceptor. Both these components then must be sites through which electrons must pass if photoresponses are to be observed. Proton transport is not involved in the generation of the photoeffects as demonstrated by the uncoupler FCCP and the ionophore valinomycin. Taking the simplest explanation, the rereduction of oxidized $BChl_2$ by cytochrome c_2 (Reaction 1) is required to prevent the back reaction and therefore ensure a sufficiently long lifetime of reduced quinone to promote forward electron transport to the electrolyte

[12]. Since we observe photocathodic responses, electrons from the chromatophore film must reduce a component in the electrolyte (either the semiquinone or *p*-quinone form in the case of hydroquinone). It is not necessary to implicate the quinone pool in electron transfer to the electrolyte, since *p*-quinone is a commonly used mediator which can directly interact with the secondary (Q_B) ubiquinone [2]. However, it is likely that the quinone pool is the acceptor for SnO_2, since it is available to the outside of the chromatophore [13] and since it represents the vast majority of acceptor molecules in the membrane.

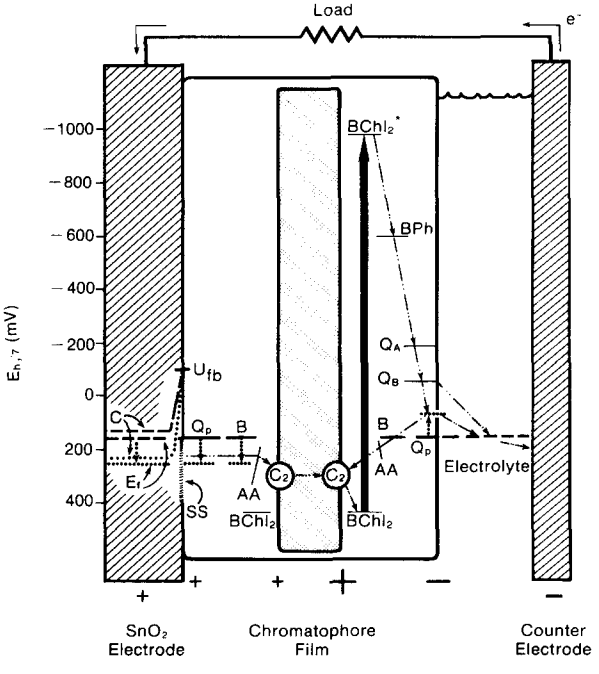

Fig. 6. Model to explain how photovoltages and photocurrents can be generated across the diameter of a chromatophore vesicle. Abbreviations: $BChl_2$, the bacteriochlorophyll dimer, primary electron donor; $BChl_2$*, the first excited singet state of $BChl_2$; BPh, bacteriopheophytin; Q_A, iron-quinone acceptor; Q_B, secondary acceptor; Q_p, quinone pool; C_2, cytochrome c_2 donor; B, cytochrome *b*; U_{fb}, flat-band potential of SnO_2 (−95 mV); C, conduction band of SnO_2; E_f, Fermi level of SnO_2; SS, SnO_2 surface states; AA, antimycin A which blocks electron transfer between B and C_2; $E_{h,7}$, redox potential scale at pH 7.0. The dotted lines indicate changes in ambient energy levels of Q_p, B, C and E_f when the light is turned on. All other energy levels within the chromatophores are depicted as midpoint potentials. Filled surface states (before the light is turned on) are depicted as parallel horizontal lines at the SnO_2/chromatophore interface. See text for an explanation of the model.

From this information and previous studies of SnO_2 electrodes coated with bacterial reaction center complexes [2], we suggest the model in Fig. 6 to explain how a chromatophore film (depicted as a single layer of chromatophores although many layers are actually present) can produce the observed photoresponses. Light drives cyclic electron transport on both the left and right sides of the chromatophore (only that on the right side is indicated in full because only the light reactions on that side contribute net energy to the system). Ejection of electrons from reduced ubiquinone into the SnO_2 on the left side is inhibited by band bending of the semiconductor conduction band, which results in an energy barrier for electrons more oxidizing than U_{fb}, the flat-band potential (for a review of semiconductor properties at electrolyte interfaces, see Ref. 14). Equilibration of reduced ubiquinone with the electrolyte on the right side promotes a net depletion of electrons from the film due to the difference in rates of electron transfer on the two sides of the chromatophore and leads to the partial oxidation of cytochrome c_2. This explains how a coated n-type semiconductor can act as a photocathode. Electrons, then, must flow from the left to the right side of the chromatophore, and one possibility is that this occurs through a cytochrome c_2 shuttle. Net electron transport thus becomes vectorial, and this leads to charge separation across the diameter of the chromatophore and ultimately across the film. As positive charge builds up at the SnO_2/chromatophore interface due to oxidation of the quinone pool, electron transfer must occur from the SnO_2 to the quinone pool (again because steady-state photocurrents are observed). The sources of these electrons are surface states on the SnO_2 which are populated up to the Fermi level (E_f in Fig. 6). Surface states, of course, equilibrate with the Fermi level of the semiconductor by tunnelling mechanisms and this completes the electrical circuit in the photoelectrochemical cell. Thus, the observed photovoltage (Fig. 2) is the light-induced difference in the electrochemical potential of the SnO_2 Fermi level relative to the redox potential of the electrolyte.

If the quinone pool is the acceptor, then electron transfer from the bulk semiconductor to the quinone pool is probably the rate-limiting reac-

tion, and this could explain the decline in photoresponse from a peak value to a lower steady-state value (Fig. 2). The rate-limiting reduction of the quinone pool would cause cytochrome c_2 to become gradually more oxidized and this would limit the amount of $BChl_2$ contributing to the photeffects (see Fig. 5). The effect of antimycin A exhibited in Table II can be explained on the basis of its inhibition of cyclic electron transport. The inhibition of cytochrome *b* oxidation on the right side of the chromatophore in Fig. 6 promotes electron transfer to the electrolyte. However, since quinone pool reduction by SnO_2 is rate limiting, one expects that on this side the effect of inhibition of quinone pool oxidation (via cytochrome *b*) by antimycin will be minimal. The result is to increase the observed photovoltage and photocurrent. The experiment in Fig. 4 is consistent with this and shows that the photocurrent rise time for a single flash is largely unaffected by antimycin, whereas the decay halftime is about doubled.

This explanation requires that the antimycin block be leaky but not rate limiting. Any alternative model would have to take into account the obligatory role for both the quinone pool and cytochrome c_2 and the effect of antimycin A.

The operation of sphericle-coated electrodes can be explained using similar arguments but taking into account the reversed orientation of the components. For example, 1,4-naphthoquinone but not 1,4-naphthoquinone-2-sulfonate increases the photoeffects with sphericles. The sulfonate cannot penetrate the membrane, whereas the simple naphtoquinone can, demonstrating the interaction of the naphthoquinone with endogenous quinones, which increases the available quinone pool and promotes the forward reaction.

This work has led to a clearer picture of the processes affecting charge transfer across coated semiconductor interfaces and across films of photosynthetic vesicles. It has also become apparent from this and previous studies with reaction center electrodes [1,2] that factors other than the orientation of the primary charge-separation transducers can play an important part in determining the net effects.

Acknowledgements

We wish to thank J. Turner, S. Lien, B. Parkinson and D. DeVault for helpful discussions. This work was supported in part by the Division of Biological Energy Research, Office of Basic Energy Sciences, U.S. Department of Energy, under Field Task Proposal 006-80.

References

1 Janzen, A.F. and Seibert, M. (1980) Nature 286, 584–585
2 Seibert, M., Janzen, A.F. and Kendall-Tobias, M. (1982) Photochem. Photobiol. 35, 193–200
3 Drachev, L.A., Kondrashin, A.A., Samuilov, V.D. and Skulachev, V.P. (1975) FEBS lett. 60, 219–222
4 Bhardwaj, R., Pan, R.L. and Gross, E.L. (1981) Nature 289, 396–398
5 Ochiai, H., Shibata, H., Fujishima, A. and Honda, K. (1979) Agric. Biol. Chem. 43, 881–883
6 Ochiai, H., Shibata, H., Souva, Y. and Katoh, T. (1980) Proc. Natl. Acad. Sci. U.S.A. 77, 2442–2444
7 Haehnel, W., Heupel, A. and Hengsterman, D. (1978) Z. Naturforsch. C 33, 392–401
8 Erabi, T., Hiura, H., Hayashi, M., Yamada, M., Endo, T., Yamoshita, J., Tanaka, M. and Horio, T., (1978) Chem. Lett. 4, 341–344
9 Dutton, P.L. and Prince, R.C. (1978) in The Photosynthetic Bacterium (Clayton, R.K. and Sistrom, W.R., eds.), pp. 525–570, Plenum Press, New York
10 Takamoto, J. and Bachman, R.C. (1979) Arch. Biochem. Biophys. 195, 526–534
11 Seibert, M, and De Vault, D. (1971) Biochem. Biophys. Acta 253, 396–411
12 Petty K.M. and Dutton, P.L. (1976) Arch. Biochem. Biophys. 172, 346–353
13 Prince, R.C., Cogdell, R.J. and Crofts, A.R. (1974) Biochem. Soc. Trans. 2, 162–164
14 Nozik, A.J. (1980) Phil. Trans. R. Soc. Lond. A. 295, 453–470